AIMS Bioengineering, 4(1): 12-27.
DOI: 10.3934/bioeng.2017.1.12
Received: 29 Novermber 2016
Accepted: 26 December 2016
Published: 30 December 2016

http://www.aimspress.com/journal/Bioengineering

Research article

Manganese orchestrates a metabolic shift leading to the increased bioconversion of glycerol into α-ketoglutarate.

Azhar A. Alhasawi and Vasu D. Appanna*

Faculty of Science and Engineering, Laurentian University, Sudbury, ON, P3E 2C6, Canada

* **Corresponding:** Email: vappanna@laurentian.ca; Tel: 705-675-1151 ext: 2112.

Abstract: Glycerol is a major by-product of the biodiesel industry and its transformation into value-added products is an ongoing technological challenge. Here we report on the ability of the nutritionally-versatile *Pseudomonas fluorescens* to synthesize copious amount of α-ketoglutarate (KG) in a glycerol medium supplemented with manganese (Mn). The enhanced production of this keto-acid was mediated by the increased activities of isocitrate dehydrogenase (ICDH)-(NAD)P dependent and aminotransaminases. At stationary phase of growth when the optimal quantity of KG was recorded, these enzymes exhibited maximal activities. Two isoforms of pyruvate carboxylase (PC) that were identified in the Mn-treated cells provided an effective route for the synthesis of oxaloacetate, a metabolite critical in the production of KG. Furthermore, the increased activities of phosphoenol pyruvate carboxylase (PEPC) and pyruvate orthophosphate dikinase (PPDK) ensured the efficacy of this KG-generating metabolic system by supplying pyruvate and ATP from the oxaloacetate synthesized by PC. Mn-exposed whole cells converted 90% of industrial glycerol into KG. This Mn-evoked metabolic network can be optimized into the economic transformation of glycerol into KG.

Keywords: bioconversion; glycerol; α-ketoglutarate; manganese; pyruvate carboxylase; metabolic networks

List of abbreviations: Manganese (Mn), α-ketoglutarate (KG), cell free extract (CFE), isocitrate dehydrogenase (ICDH), pyruvate carboxylase (PC), phosphoenolpyruvate carboxylase (PEPC), pyruvate orthophosphate dikinase (PPDK), pyruvate kinase (PK), tricarboxylic acid (TCA), aspartate aminotransferase (AST), glycine transaminase (GT), glutamate dehydrogenase (GDH),

aconitase (ACN) and spent fluid (SF).

1. Introduction

The search for renewable energy triggered by environmental concerns and the finite nature of oil reserves have propelled scientists to seek alternative technologies aimed at transforming biomass into fuels [1,2]. Bio-based processes are the most widely utilized technology in the generation of such combustible energy sources as ethanol, butanol and propanol [3]. Microbial systems have been tailored to produce these fuels from plant-derived biomass like starch or cellulose [4,5]. In this instance, following the liberation of glucose, a reaction mediated by the enzyme amylase or cellulase, the monosaccharide is subsequently converted to the desired end product. The enhanced formation of the intermediary metabolites like pyruvate, acetate and acetyl CoA is critical to the economic success of these microbial nano-factories [6,7]. The liberation of energy-rich gases H_2 and CH_4 from biomass is another avenue being pursued to satisfy the global need for clean energy as is the production of biodiesel [8,9].

In the biodiesel industry, plant or animal-derived triglycerides are the starting material that are converted to fatty acids. These fatty acids can then be either esterified or decarboxylated to hydrocarbons and utilized as fuels. One of the major draw-back of the biodiesel industry is the generation of glycerol as a by-product [10]. Indeed approximately 10% (w/w) of this trihydroxylated moiety is released and it is projected that this problem will exacerbate as the global demand for biodiesel increases. Hence, it is critical that this waste product be converted into value-added commodities if the biodiesel industry is to be economically viable. Currently, chemicals such as propane 1,3-diol, succinic acid and citric acid are among some of the microbially-mediated products that are synthesized [11,12,13].

In this study we have utilized the metabolically-versatile soil microbe *Pseudomonas fluorescens* to transform glycerol into KG. Metabolic engineering is an important strategy that can aid in fine-tuning the precise molecular pathways responsible for the transformation of this trihydroxy alcohol into products of economic significance. Although genetic manipulation may be utilized to modulate metabolic activities in order to induce the formation of a desired metabolite, micro-nutrients like manganese can also promote significant metabolic shift leading to value-added products [14,15]. This divalent metal is required for the optimal activity of a variety of enzymes including pyruvate carboxylase (PC), phosphoglyceromutase (PG), pyruvate kinase (PK), and phosphoenol pyruvate carboxylase (PEPC) that are central to the metabolism of glycerol [16,17]. Manganese-dependent enzymes are also pivotal in combatting oxidative stress and in the metabolic networks involved in the transformation of carbohydrates [18,19]. In fact, the ability of this element to promote exopolysaccharide production in micro-organisms has been attributed to its close ionic similarity to magnesium, an avid cation for monosaccharides and their phosphorylated derivatives [20]. Some microbes have been shown to produce KG, a metabolite of significant industrial applications from different carbon sources [21]. However, this is the first demonstration of ability of Mn to elicit a metabolic reconfiguration resulting in the enhanced formation of this dicarboxylic acid from industrial glycerol. Here we report on the influence of this divalent metal on glycerol metabolism in

P. fluorescens and on various enzymes responsible for enhanced synthesis of KG. The metabolic pathways mediating the fixation of the trihydroxy alcohol into oxaloacetate and its eventual conversion into KG are delineated. Furthermore, the effectiveness of the Mn-evoked transformation of industrial glycerol into this keto-acid by intact microbial cells is also discussed.

2. Materials and Methods

2.1. Bacterial culturing techniques and biomass measurement

The bacterial strain *Pseudomonas fluorescens* 13525 from American Type Culture Collection (ATCC) was grown in a mineral medium containing (per liter of deionized water) Na_2HPO_4 (6.0 g); KH_2PO_4 (3.0 g); NH_4Cl (0.8 g); and $MgSO_4$ (0.2 g). Trace elements (1 mL) were added as previously described [22–25]. The pH was adjusted to 6.8 with the addition of 2 N NaOH. Glycerol (10% v/v : 1.37 M) from Sigma Aldrich (Oakville, Canada) was added to the medium as the sole source of carbon. Prior to inoculation, the media were dispensed in 200 mL aliquots in 500 mL Erlenmeyer flasks. Various concentrations of $MnCl_2$ ranging from 25 μM to 1 mM were utilized to optimize the conditions for maximal production of KG. The media were inoculated with 1 mL of stationary phase cells (450 μg protein equivalent) of the control culture and were then incubated at 26 °C in a gyratory water bath shaker, model 76 (New Brunswick Scientific) at 140 rpm. Cells were harvested at different time intervals by centrifugation at 10,000×*g* for 20 min. The bacterial pellets were treated with 1 mL of 1 N NaOH and the biomass was measured with the aid of the Bradford assay [26]. The spent fluid (SF) was analyzed by a variety of techniques. All comparative studies were done with cells at the same growth phases i.e. 40 h for the controls and 48 h for the Mn-treated cells.

2.2. Regulation experiments and cellular fractionation

To confirm if the metabolic changes were indeed induced by the addition of Mn, control cells were added to Mn-treated media while cells isolated from the Mn cultures were incubated in control media. To afford an accurate comparison, these cells were gathered at the same growth phase. Following their incubation at 26 °C for 6 h in a gyratory water bath, the cells were harvested as aforementioned. The cellular fractions were isolated by centrifugation and assayed for select enzymatic activities. The spent fluid was removed for further analysis and the pellet was washed with 0.85% NaCl (10 mL). Cells were then resuspended in a cell storage buffer (pH 7.3) containing [50 mM Tris-HCl; 5 mM $MgCl_2$ and 1 mM phenylmethylsulfonylfluoride (PMSF)] and disrupted by sonication using a Brunswick Sonicator on power level 4 for 15 sec 4 times and with 5 min pauses. To obtain the cell free extracts [(CFE) soluble and membranous fractions], cells were centrifuged for 3 h at 180,000×*g* at 4 ^{o}C. Unbroken cells were initially removed by centrifugation at 10,000×*g* for 20 min. The Bradford assay was performed in triplicate to determine the protein concentration of both fractions using bovine serum albumin (BSA) as the standard [26].

2.3. Metabolite analysis

Metabolite levels were monitored by high performance liquid chromatography (HPLC). Soluble cell free extract (CFE) was taken immediately in order to minimize any degradation and then boiled for 10 min to precipitate proteins before analysis. Quenching with 60% methanol afforded similar results [27]. Samples of spent fluid and CFE were injected into an Alliance HPLC equipped with a C18 reverse-phase column (Synergi Hydro-RP; 4 μm; 250 × 4.6 mm, Phenomenex) operating at a flow rate of 0.7 mL/min at ambient temperature and Waters dual absorbance detector were utilized as described in [27]. Activity bands obtained by electrophoresis were excised from the gel and placed in a reaction mixture containing 2 mM substrates. After 30 min of incubation, 100 μL of the sample was removed and diluted with Milli-Q water for HPLC analysis. Mobile phase containing 20 mM KH_2PO_4 (pH 2.9) was used at a flow rate of 0.7 mL/min at ambient temperature to separate the substrates and products, which were measured at 210 nm to detect carbonyl groups and 280 nm to identify nucleic acids. To ensure the metabolite identity biological samples were spiked with known standards, and peaks were quantified using the Empower software (Waters Corporation). In order to assess the biotechnological potential, the whole cells (4 mg protein equivalent) collected at the same phase of growth were incubated in 10% glycerol (commercial and industrial, ROTHSAY biodiesel company, Ontario, Canada) media devoid of NH_4Cl for various times (0 h, 3 h, 6 h and 24 h) and the production of KG was monitored both by HPLC and the 2, 4 dinitrophenyl hydrazine (DNPH) assay [28]. The consumption of glycerol was monitored colorimetrically as described [29].

2.4. Spectrophotometric analysis of various enzymes and α-ketoglutarate determination assay

Spectrophotometric data for ICDH-NAD/NADP activity were achieved by incubating 0.1 mg protein equivalent of membrane or soluble CFE from control and Mn-treated cells in reaction buffer containing (25 mM Tris-HCl, 5 mM $MgCl_2$, pH 7.4) with 2 mM isocitrate. NAD or NADP (0.5 mM) was utilized as the cofactor and the reaction mixtures were monitored for 3 min for NAD(P)H production at 340 nm. Negative controls were accomplished without the substrates or cofactors. The activity of aconitase (ACN, EC 4.2.1.3) was determined in the soluble fractions of the CFE. Tricarballylic acid (10 mM), a citrate analogue was added to the whole cells prior to cellular disruption to ensure the stability of this enzyme [30]. The assay consisted of activity buffer (25 mM Tris-HCl, 5 mM $MgCl_2$, pH 7.4), 10 mM substrate (citrate) and 200 μg/mL soluble protein. The reaction was monitored at 240 nm for the formation of cis-aconitate as previously described. Aconitate served as the standard and specific activities were calculated. Blanks were prepared in a similar fashion however, substrate or protein was omitted from the mixture [30].

The carbonyl group of ketoacids were readily measured by DNPH assay [28]. Spent fluid obtained from control and Mn-cultures at different time intervals were monitored. Absorbance was measured at 490 nm and concentrations were calculated using α-ketoglutarate as the standard. Following a 10-fold dilution, glycerol concentration in the spent fluid was also assessed [29]. Commercial glycerol [Sigma Aldrich (Oakville, Canada)] was the standard.

2.5. Monitoring enzymatic profiles by BN-PAGE

Blue native polyacrylamide gel electropohoresis (BN-PAGE) was accomplished as described [31,32,33]. Briefly, membrane and soluble fractions were isolated and prepared in a non-denaturing buffer (50 mM Bis-Tris, 500 mM ε-aminocaproic acid, pH 7.0, 4 °C) at a concentration of 4 μg/μL. For membrane solubilisation, 10% maltoside was included in the buffer A, 4–16% gradient gel was prepared with the Bio-Rad MiniProteanTM 2 system using 1 mm spacers to afford optimal protein separation. Sixty micrograms of proteins were loaded into each well prior to electrophoresis under native conditions at 80 V to ensure proper stacking, then at 300 V for proper migration through the gel. The blue cathode buffer [50 mM Tricine, 15 mM Bis-Tris, 0.02% (w/v) Coomassie G-250 (pH 7) at 4 °C] was used to aid visualize the running front and was exchanged to a colorless cathode buffer (50 mM Tricine, 15 mM Bis-Tris, pH 7 at 4 °C) when the running front was halfway through the gel. Upon completion, the gel was equilibrated in the reaction buffer for 15–30 min. The in-gel visualization of enzyme activity was determined by associating the formation of NAD(P)H to 0.2 mg/mL of phenazine methosulfate (PMS) and 0.4 mg/mL of iodonitrotetrazolium (INT), or by coupling the formation of NAD(P) to 16.7 μg/mL, 2,6-dichloroindophenol (DCPIP) and 0.4 mg/mL INT. Isocitrate dehydrogenase (NAD or NADP) was analyzed in-gel with a reaction mixture consisting of 5 mM isocitrate, 0.5 mM NAD(P), 0.2 mg/mL of PMS and 0.4 mg/mL of INT. Aspartate transaminase (AST) was incubated in equilibrium buffer, 5 mM KG, 5 mM aspartate, 5 units of glutamate dehydrogenase (GDH), 0.5 mM NAD, 0.2 mg/mL PMS and 0.4 mg/mL INT [27]. Glycine transaminase (GLT) was monitored as described with the aid of lactate dehydrogenase in order to visualize glyoxylate production [34]. Glutamate dehydrogenase (GDH) was tracked using a reaction buffer with 5 mM glutamate, 0.5 mM NAD, 0.2 mg/mL PMS and 0.4 mg/mL INT. For pyruvate carboxylase (PC) analysis, the membrane CFE was electrophoresed and was incubated with 5 mM pyruvate, 0.5 mM ATP, 0.5 mM HCO_3^- 10 units of malate dehydrogenase (MDH), 0.5 mM NADH, 16.7 μg/mL DCPIP and 0.4 mg/mL INT. The product oxaloacetate was traced with assistance of MDH. Bromopyuvate was used as the inhibitor of PC [35]. α-Ketoglutarate dehydrogenase (KGDH) was monitored by using 5 mM KG, 0.5 mM CoA, 0.5 mM NAD, 0.2 mg/mL PMS and 0.4 mg/mL INT [36]. Pyruvate dehydrogenase (PDH) activity was tracked with the reaction buffer consisting of 5 mM pyruvate, 0.1 mM CoA, 0.5 mM NAD, 0.2 mg/mL PMS and 0.4 mg/mL INT [36]. PEPC, PPDK and PK activities were visualized as described previously [33,37]. In this instance, the formation of oxaloacetate and pyruvate were detected with MDH and LDH respectively. Complex IV was examined by the addition of 10 mg/mL of diaminobenzidine, 10 mg/mL cytochrome C, and 562.5 mg/mL of sucrose [33]. To ensure equal protein loading, the gels were stained by Coomassie blue G-250. Enzymes like GDH and complex IV that had relatively similar activities in both cultures were also utilized in order to confirm that equal quantities of proteins were being electrophoresed. The activity of select enzymes including ICDH-NADP (2 mM isocitrate and 0.5 NADP for 30 min), PC (2 mM pyruvate, 0.5 ATP and 2 mM HCO_3^- for 30 min), PPDK (2 mM PEP and 1 mM AMP and 0.5 mM PPi) PC/AST were incubated in reaction buffer containing (2 mM glutamate, 2 mM pyruvate and 2 mM HCO_3^-) and the isozymes for PC were further confirmed by incubating the activity bands with the appropriate substrates and monitoring the products by HPLC. Inhibitors like 5 mM rotenone for complex I and 5 mM bromopyruvate for PDH and PC were utilized to confirm the specificity of the desired enzymes.

Reactions were stopped using a destaining solution (40% methanol, 10% glacial acetic acid) once the activity bands had reached the necessary intensity. Reactions performed without the addition of a substrate or cofactor or inhibitor in the reaction mixture ensured specificity. Densitometry was performed using Image J for Windows.

2.6. Pyruvate metabolism by select enzymes monitored by NMR and HPLC

To establish if indeed these enzymes were a source of oxaloacetate, pyruvate and ATP, the activity bands attributable to these enzymes were added sequentially to the substrates and the products were assessed. 13C-NMR analyses were accomplished using a Varian Gemini 2000 spectrometer operating at 50.31 MHz for 13C. Samples were analyzed with a 5 mm dual probe (35 u pulse, 1-s relaxation delay, 8 kilobytes of data, and 3000 scans). Chemical shifts were confirmed by comparing to standard compounds under analogous conditions [38]. The formation of oxaloacetate was first investigated by incubating the excised band of PC from the membrane CFE of Mn cultures for 1 h in phosphate reaction buffer containing (2 mM pyruvate labelled 13C-3, 0.5 mM ATP, 10 mM HCO_3^-). The reaction was stopped by removing the excised gel and heating at 60 °C. Following the identification of the labelled oxaloacetate peak, it was incubated with the excised band corresponding to the activity of PEPC and PPDK [Note: These bands were localized at the same spot in the gel and AMP (0.5 mM) was added to this incubation mixture]. Once, the reaction was complete, the products were analysed by NMR and HPLC. The metabolites were identified by comparing to known standards. As PC and AST activities located in the membrane CFE co-migrated on the gel, the activity band was excised and incubated with 2 mM pyruvate, 0.5 mM ATP, 10 mM HCO_3^- and 2 mM glutamate for 1 h. The formation of KG oxaloacetate and aspartate was monitored by HPLC.

2.7. Statistical analysis

Data were expressed as means ± standard deviations (SD). Statistical correlations of the data were checked for significance using the Student t test (*$p \leq 0.05$, ** $p \leq 0.01$). All experiments were performed at least twice and in triplicate.

3. Results

3.1. Influence of manganese on cellular growth and metabolite profile

P. fluorescens was able to grow in a mineral medium with 10% glycerol. However, in the cultures supplemented with Mn, there was a distinct difference in the nature and levels of metabolites in these cultures. The spent fluid from the Mn-cultures was characterized with prominent peaks indicative of KG and succinate (Figure 1A). The inclusion of 50 μM Mn in the growth medium elicited the production of maximal amount of KG. At least a 4-fold increase in KG was observed compared to the controls. A marked diminution was observed at lower and higher concentrations of Mn (Figure 1B). As 50 μM Mn evoked the optimal response, this concentration was utilized to decipher the metabolic networks responsible for the enhanced production of the keto-acid. Although the rate of growth was slightly slower in the Mn-media, at the stationary phase of growth the cellular

yield was similar to that observed in the control cultures (Figure 1C). The concentration of KG in the spent fluid as monitored by DNPH assay in the Mn-cultures increased with the time of incubation and was found to be maximal at stationary phase of growth (Figure 1D). There was no significant difference in the consumption of glycerol in these cultures. At stationary phase of growth almost 90% of this carbon source was utilized in the control and Mn-supplemented media. The pH at stationary phase of growth was 6.0 most likely due to secretion of KG. To elucidate the metabolic networks responsible for this seminal observation, the select metabolite profile of the soluble CFE was analyzed. Although peaks attributable to KG, pyruvate, isocitrate, oxaloacetate, succinate and ATP were evident, there was a marked variation in the levels of isocitrate, oxaloacetate and succinate in the Mn-grown cells compared to the cells obtained from the control cultures (Figure 2A). This observation prompted the analysis of complex IV, an enzyme critical in energy production via oxidative phosphorylation. There was no significant variation in the activity of this enzyme in both cultures; the activity of complex I also did not appear to be influenced by the presence of Mn in the medium (Figure 2B). PDH, an enzyme that supplies acetyl CoA and is inhibited by bromopyruvate was relatively similar in both cultures (Figure 2C).

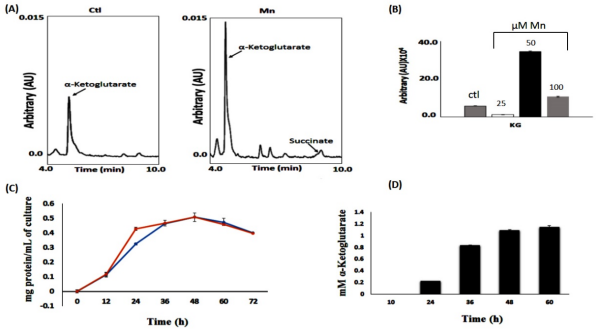

Figure 1. Influence of Mn on KG production. (A) HPLC analyses of spent fluid in control and Mn cultures (B) KG production at different Mn concentrations (C) Growth profile of *P. fluorescens* grown in 10% glycerol with 50 μM Mn. The black curve indicates Mn cultures; the grey curve control culture (D) KG concentrations in spent fluid at various time intervals in Mn-cultures (50 μM). (n = 3).

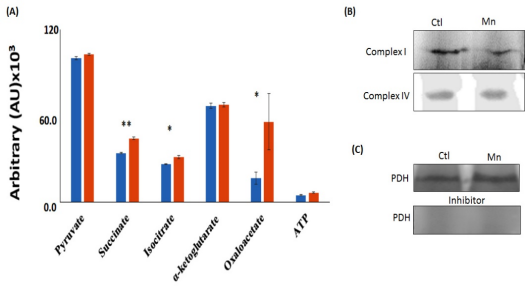

Figure 2. Functional metabolomics and select energy-producing enzymes. (A) HPLC of targeted metabolites from control and Mn-treated cells (at stationary phase of growth) (B) Enzymes involved in oxidative phosphorylation (complex I and IV) (C) Pyruvate dehydrogenase activity with and without inhibitor (Gels are representative of 3 experiments; Ctl = control, Mn-treated).

3.2. Enzymes involved in KG homeostasis

As KG was a major metabolite generated in the presence of Mn, various enzymes involved in the homeostasis of this ketoacid were monitored. There was a significant increase in activities of such enzymes as ICDH-NAD as well as ICDH-NADP (Figure 3A, B). In fact, three isoenzymes of ICDH-NAD were visualized by the in-gel activity assay. These were confirmed by incubating the appropriate sections of the gel separately in the substrates and monitoring the products. ICDH-NADP activity band was excised and treated with the isocitrate and NADP in order to monitor the production of KG by HPLC (Figure 3C). Spectrophotometric assays revealed at least a 2-fold increase in ICDH-NADP activity (Table 1). These enzymes were also monitored at different growth intervals and maximal activity was observed at the stationary phase of growth for both ICDH-NADP/NAD (Figure 3D). (Note that the activity at the earlier periods was evident only if the gel was incubated in the substrate for longer time). In order to verify if indeed this increase in enzymatic activity was due to the presence of Mn, control cells were incubated in the Mn-media and Mn-grown cells were exposed to the control culture conditions. A reversal of ICDH activities was observed (Figure 3E). Hence, the dependence of the increased activity of this enzyme on Mn was evident. α-Ketoglutarate dehydrogenase (KGDH), a TCA cycle enzyme involved in the decarboxylation of KG was shown to have diminished activity in the cells harvested from the Mn-media compared to the control cells (Figure 3F). Aconitase (ACN), an enzyme referred to as the gate-keeper of the TCA cycle was increased 2-fold in activity in the Mn-supplemented media (Table 1).

Table 1. Various enzymatic activities in cell-free extracts from control and Mn-treated *P. fluorescens* at the same growth phase.

Enzymes	Control	Mn
NAD^+-dependent isocitrate dehydrogenase [a]	0.64 ± 0.07	1.07 ± 0.11*
$NADP^+$-dependent isocitrate dehydrogenase [a]	0.4 ± 0.014	0.84 ± 0.009*
Pyruvate carboxylase[b]	0.57 ± 0.09	1.2 ± 0.24*
Aconitase[c]	11 ± 0.1	22 ± 0.5*

[a] μmol NAD(P)H produced min^{-1} mg $protein^{-1}$ as monitored at 340 nm (n = 3 ± standard deviation).

[b] μmol NADH consumed min^{-1} mg $protein^{-1}$ as monitored at 340 nm (n = 3 ± standard deviation).

[c] Specific activity of aconitase (μmol of aconitate consumed min^{-1} mg $protein^{-1}$ monitored at 240 nm) (n = 3 ± standard deviation).

*Denotes a statistically significant differences compared with the control ($P \leq 0.05$).

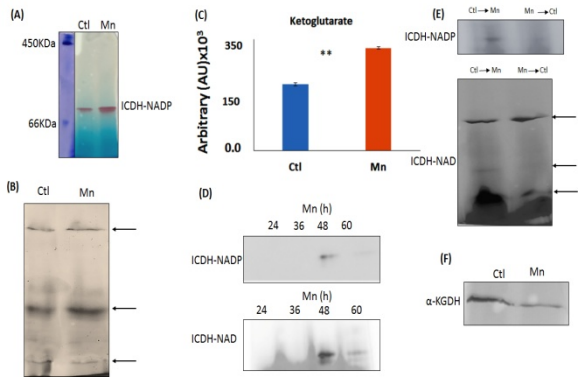

Figure 3. KG homeostasis in *P. fluorecens* grown in 10% glycerol. (A) In-gel enzymatic activity of isocitrate dehydrogenase (ICDH-NADP), Ferritin (450 KD) and BSA (60 KDa) (B) In-gel enzymatic activity of isocitrate dehydrogenase (ICDH-NAD) (C) HPLC analysis of excised band (A) incubated in 2 mM isocitrate, 0.5 mM NADP for 30 min (D) Time profile (h) of ICDH-NAD/NADP activities (E) In-gel activity of ICDH-NAD/NADP when control cells were incubated in Mn-cultures and Mn-treated cells were exposed to control media (F) In-gel KGDH activity. (Gels are representative of 3 independent experiments. Ctl = Control; Mn-treated).

3.3. The role of PC in oxaloacetate and PEP formation

For this organism to proliferate in glycerol, the 3-carbon nutrient has to be transformed into oxaloacetate, a moiety essential for the TCA cycle and gluconeogenesis. Pyruvate carboxylase (PC) a Mn-dependent enzyme that orchestrates the carboxylation of pyruvate into oxaloacetate with ATP as the cofactor would be a good candidate. This enzyme was characterized with elevated activity and two activity bands indicative of two isozymes that were associated with the cells grown in the Mn-enriched media (Figure 4A). Incubation of excised bands with pyruvate, HCO_3^-, and ATP yielded an oxaloacetate peak as revealed by HPLC. This metabolite was further confirmed enzymatically with the aid of malate dehydrogenase and NADH (data not shown). PC had a maximal activity at 48 h, a growth phase corresponding to the optimal production of KG (Figure 4A).

As phosphoenol pyruvate (PEP) is an important precursor to the synthesis of pyruvate, the activity of PEPC, an enzyme responsible for the transformation of oxaloacetate to PEP was analyzed. The activity band was more intense in the cells obtained from the Mn-supplemented media. Furthermore, the presence of an isozyme was also detected (Figure 4B). The PEP was readily converted to pyruvate by PPDK and PK as these enzymes were associated with markedly increased activity bands in the soluble CFE from the Mn-exposed cells compared to the control (Figure 4B). To establish if PC, PEPC and PPDK may be working in tandem, the fate of labelled pyruvate (13C-3) and ATP was monitored. Following the formation of 13C labelled oxaloacetate by the PC activity band, this substrate was incubated with PEPC and PPDK band in the presence of AMP and PPi. The production of pyruvate and ATP were followed. Indeed this metabolic module fixed CO_2, produced oxaloacetate and regenerated pyruvate and ATP (Figure 4C). The enhanced synthesis of oxaloacetate in the Mn-cultures propelled by PC may not only be an important contributor to ATP production via the formation of PEP but may help transform glutamate into KG.

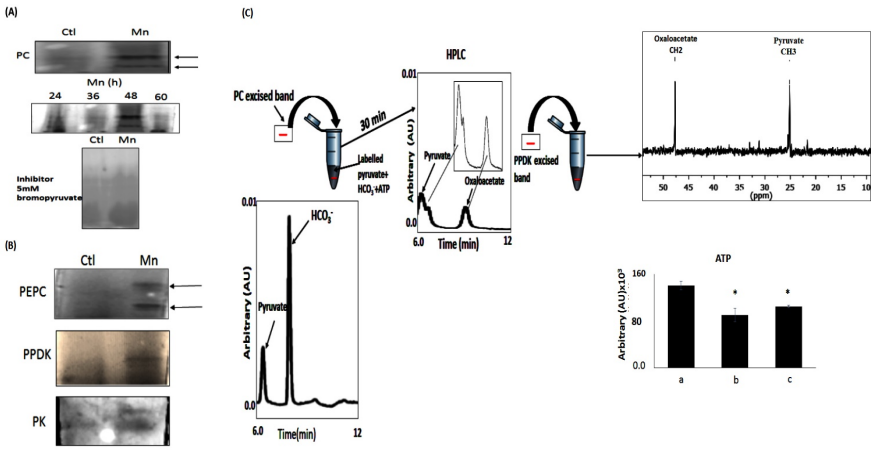

Figure 4. Pyruvate metabolism and ATP production. (A) In-gel activity of pyruvate carboxylase (PC), activity at various time intervals and activity in the presence of inhibitor (5 mM bromopyruvate) (B) Phosphoenolpyruvate carboxylase (PEPC), pyruvate orthophosphate dikinase (PPDK) and pyruvate kinase (PK) activity BN-PAGE (C) HPLC and NMR analyses of excised PC activity band (membrane CFE) and PEPC/PPDK activity band (soluble CFE) (Note: oxaloacetate produced in the first reaction was incubated with PEPC/PPDK band in the presence of AMP and PPi). (Note: NMR peak corresponding to CH_2 in oxaloacetate; ATP was monitored at time = 0) a) then following the incubation with the PC band; b) and after reaction with PPDK/PEPC band in the presence of AMP; c) Note: ATP data were analysed by one-way ANOVA for the significance. Gels are representative of 3 independent experiments. Ctl = Control; Mn-treated.

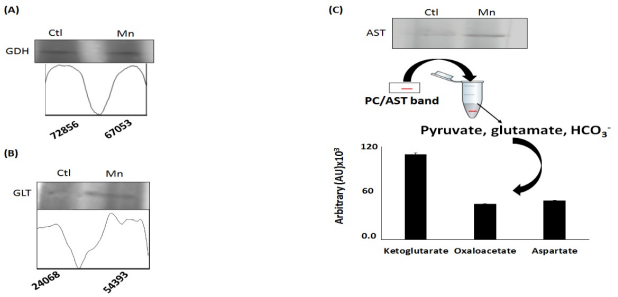

Figure 5. Glutamate-metabolizing and KG-producing enzyme activities by BN-PAGE and HPLC (A) Glutamate dehydrogenase (GDH) and densitometric reading of activity band (B) Glycine transaminase (GLT) and densitometric reading of activity band (C) Aspartate aminotransminase (AST) and HPLC analyses of excised band incubated with 2 mM glutamate, pyruvate and HCO_3^-. Note: the formation of KG; Gels are representative of 3 independent experiments; PC and AST bands co-migrated. Ctl = Control; Mn-treated. Densitometry was performed using Image J for windows.

Since transaminases and GDH play a role in the homeostasis of KG, these enzymes were monitored. AST and GLT were found to be elevated while GDH did not change significantly in the

cells isolated from the Mn-cultures (Figure 5A, B, C). As the lower PC band and AST co-migrated during the BN-PAGE, this band was excised. As it was harbouring these enzymes, its ability to form KG from pyruvate, glutamate, ATP and HCO_3^- was evaluated. Peaks indicative of KG, oxaloacetate and aspartate were obtained (Figure 5C).

3.4. Mn-treated cells and biotransformation of industrial glycerol into KG

As the SF and CFE extract from the Mn cells were characterized by copious amounts of KG, it was essential to assess the ability of the intact cells to produce this value-added metabolite from glycerol. The whole cells were incubated in phosphate media devoid of a nitrogen source and at various time intervals, cells were centrifuged and KG was monitored using DNPH. After 24 h of incubation, the intact Mn-treated microbes synthesized approximately 1.2 mM KG from the industrial glycerol compared to 0.12 mM from the glycerol purchased from Sigma (Figure 6A). After 24 h of incubation, the Mn whole cells consumed 90% of the industrial starting material obtained from ROTHSAY, Canada compared to 60% of the commercial one (data not shown).

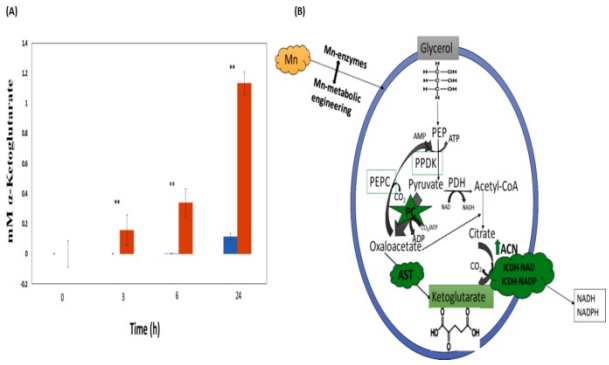

Figure 6. KG production by intact cells and Mn-dependent metabolic engineering involved in KG synthesis. (A) KG formed when whole cells were incubated with commercial and industrial glycerol [Note: 60% and 90% of glycerol were consumed in the commercial (Sigma) and industrial (ROTHSAY, Canada) respectively, SD ± 2.0%, n = 3] (B) Scheme depicting a PC-propelled metabolic reconfiguration mediating the production of KG in *P. fluorescens* exposed to Mn. (Green indicates an increase).

4. Discussion and Conclusion

The foregoing data point to the ability of *P. fluorescens* to produce KG from glycerol in the presence of Mn. The metabolic re-engineering elicited by the interaction of the microbe with Mn exposes an intriguing strategy of how microbial systems can be coached to perform a desired commercial task. This divalent metal is involved in a variety of enzymatic reactions contributing to the metabolism of carbohydrates, in the fixation of CO_2, in anti-oxidative defence and in the carboxylation processes [16,39–41]. Pyruvate carboxylase is a Mn-dependent enzyme and is responsible for the addition of CO_2 to pyruvate with the concomitant formation of oxaloacetate. This reaction utilizes ATP as the co-factor [42,43]. The overexpression of the PC gene in a yeast has been shown to elicit the maximal secretion of this ketoacid when glycerol was the source of carbon [44]. In this present study the expression of the two PC isozymes appeared to play a critical role in the

enhanced production of KG observed when Mn was included in the cultures. The activity of PC was optimal at 48 h of growth, a time that corresponded with the ability of the microbe to produce the maximal amounts of KG from glycerol. Since Mn was readily available, it is quite likely that the presence of the divalent metal in the medium may have promoted the expression of these isozymes. Metal-dependent proteins are intricately regulated and the availability of the metal tends to be a critical ingredient in this process [45]. As 50 μM Mn enabled the microbe to produce the most KG, it is within the realm of possibility that this concentration of the divalent metal may be evoking the optimal enzymatic activity. Indeed Mn is known to be toxic when present in elevated amounts. Depending on its concentration this divalent metal can be either essential or a toxin [46]. The decrease in activity at higher Mn concentration may be attributed to its dose-dependent toxicity.

Oxaloacetate a key intermediate in a variety of metabolic networks may undergo numerous transformations in order to fuel the synthesis of KG. Aspartate transaminase (AST) is known to readily effect the conversion of glutamate and oxaloacetate into KG and aspartate [27]. The activity of this enzyme was elevated in the cells harvested from the Mn-supplemented cultures. These two enzymes (PC/AST) co-migrated in the gel and the excised activity band yielded KG upon incubation with pyruvate, HCO_3^- and glutamate. This molecular arrangement would permit the funnelling of oxaloacetate to the production of KG. Indeed, the transient assemblage of enzymes dedicated to the synthesis of a desired product is a common biochemical phenomenon that facilitates the production of a select metabolite. Recently it was shown that the close proximity of citrate lyase, PEPC and PPDK allowed the survival of *P. fluorescens* challenged by nitrosative stress. This partnership among the enzymes enabled the production of ATP in an O_2-independent manner as oxidative phosphorylation was ineffective [33]. In this instance the shuttling of PC-generated oxaloacetate towards the proximal AST would ensure the efficacy in the production of KG. The enhanced activity of glycine transaminase (GLT) observed in the Mn cultures, would also add to KG budget. Oxaloacetate is also a critical precursor of citrate synthesis, a reaction that is aided by a constant supply of acetyl CoA. Pyruvate dehydrogenase (PDH) activity was prominent in the Mn-treated cells as was the activity of aconitase (ACN). However, the enzymes mediating the decarboxylation of isocitrate into KG, a metabolite with numerous biological functions [47] were sharply enhanced in the Mn-enriched cultures. Indeed, both ICDHs, the NAD and NADP dependent were markedly elevated. The ICDH-NAD dependent was evident as three isozymes. The overexpression of this enzyme in microbial systems has been utilized to promote the synthesis of KG from glycerol [33]. The diminished activity of KGDH may be also contributing to the accumulation of KG, an enzyme with diminished activity in the cells harvested from the Mn-cultures. The enhanced activity of ICDH coupled with the concomitant diminution in the activity of KGDH may be an important stratagem this microbe may be resorting to in order to accumulate KG.

The enhanced activity of PC may not only be a source of the crucial oxaloacetate but may be also aiding in fulfilling the need for ATP. In this study, complex IV that mediates the final electron transfer step during ATP production by oxidative phosphorylation did not appear to be significantly affected. However, the demand for ATP by PC may have compelled the microbe to complement its energy-generating machinery by activating the substrate-level phosphorylation pathway. As oxaloacetate was abundantly being supplied by the overexpression of the Mn-dependent PC, the microorganism was readily tapping this ketoacid into the formation of the high-energy, PEP. This conversion catalyzed by PEPC is quite energy efficient as it necessitates inorganic phosphate (Pi) as the co-factor. The subsequent decarboxylation of oxaloacetate yields PEP that can be readily fixed

into ATP in the presence of either ADP or AMP; pyruvate is produced as a consequence of this reaction. PPDK that uses AMP as the nucleotide was elevated in the cells isolated from the Mn cultures. This enzyme is known to provide organisms an adaptive advantage to survive conditions where oxidative phosphorylation is compromised due to oxidative stress, lack of oxygen, deficiency in iron or assault by macrophages [33,27,48]. In this instance, other than augmenting the energy budget of the microbe, this metabolic network may also be contributing to pyruvate homeostasis, a pivotal feature in the Mn-induced KG accumulation in *P. fluorescens.* This ketoacid fuels the fixation of CO_2 into oxaloacetate by PC, an enzyme whose expression and activity are responsive to Mn [16,42,49].

The seminal experiments with the membrane localized PC and the soluble cellular component with PEPC and PPDK where oxaloacetate, and ATP were produced provided compelling evidence that these enzymes may be working in tandem. Furthermore the regeneration of the initial 13C-3 labelled pyruvate vividly illustrates that this organism may be utilizing this metabolic network not only to produce oxaloacetate but also to synthesize ATP. It is also within the realm of possibility to argue for the notion that Mn has compelled *P. fluorescens* to fix CO_2 in the presence of glycerol to fulfill its energy and metabolic needs. By invoking this process, the organism has abundant access to oxaloacetate and ATP. The former can be readily transaminated in order to produce KG and converted to citrate, a critical precursor to KG via isocitrate. Since one of the objectives of this investigation was to generate value-added products from glycerol, a waste from the biodiesel industry, the ability of intact cells to transform this trihydroxy alcohol into KG was evaluated. The maximal KG was obtained after 24 h of incubation and industrial glycerol yielded more ketoacid compared to the commercial variety. Although further investigation needs to be undertaken in order to unravel the commercial application of these findings, it is not unlikely that the composition of these starting materials may be the contributing factor. Manganese supplementation provides a relatively facile operation aimed at triggering a plethora of metabolic networks dedicated to the production of KG.

In conclusion, this work reveals the significance of abiotic change in modulating biochemical behaviour. The presence of Mn has a profound influence on glycerol metabolism leading to the accumulation of KG. The overexpression in the activities of such Mn-requiring enzymes as PC, PPDK and PEPC provides an effective route to oxaloacetate and ATP. The former was an important source of KG, a value-added product that was made easily accessible due the enhanced activities of transaminases and ICDH (Figure 6B). The metabolic shift prompted by Mn presents a relatively facile stratagem to program microbes to execute assignments of economic importance. These metabolic networks evoked by Mn provide a relatively inexpensive means of synthesizing KG from glycerol. This is the first demonstration of a metabolic reprogramming involving the synthesis of oxaloacetate, acetyl CoA and ATP, three ingredients propelling the enhanced production of KG from industrial glycerol. Optimization of these biochemical processes has the potential of yielding biofactories that may assist the biodiesel industry to be more profitable and environmentally neutral.

Acknowledgment

This study was funded by Laurentian University and the Northern Ontario Heritage Fund. Azhar Alhasawi is a recipient of funding from the Ministry of Higher Education of Saudi Arabia.

Conflict of Interest

All authors declare that they have no conflict of interest.

References

1. Kumar M, Gayen K (2011) Developments in biobutanol production: new insights. *Appl Ener* 88: 1999–2012.
2. Hoekman SK (2009) Biofuels in the US-challenges and opportunities. *Renew Ener* 34: 14–22.
3. Behera S, Singh R, Arora R, et al. (2014) Scope of algae as third generation biofuels. *Front Bioeng Biotechnol* 2: 90.
4. Saxena RC, Adhikari DK, Goyal HB (2009) Biomass-based energy fuel through biochemical routes: a review. *Renew Sust Energ Rev* 13: 167–178.
5. Ullah K, Ahmad M, Sharma VK, et al. (2014) Algal biomass as a global source of transport fuels: overview and development perspectives. *Prog Nat Sci Mater Int* 24: 329–339.
6. Elkins JG, Raman B, Keller M (2010) Engineered microbial systems for enhanced conversion of lignocellulosic biomass. *Curr Opin Biotechnol* 21: 657–662.
7. Papagianni M (2012) Recent advances in engineering the central carbon metabolism of industrially important bacteria. *Microb Cell Fact* 11: 1–13.
8. Liao J, Mi L, Pontrelli S, et al. (2016) Fuelling the future: microbial engineering for the production of sustainable biofuels. *Nat Rev Microbiol* 14: 288–304.
9. Suero SR, Ledesma B, Álvarez-Murillo A, et al. (2015) Glycerin, a biodiesel by-product with potentiality to produce hydrogen by steam gasification. *Energies* 8: 12765–12775.
10. Luna C, Verdugo C, Sancho ED, et al. (2014) Production of a biodiesel-like biofuel without glycerol generation, by using Novozym 435, an immobilized *Candida antarctica* lipase. *BRBP* 1: 1–11.
11. Da Silva GP, Mack M, Contiero J (2009) Glycerol: a promising and abundant carbon source for industrial microbiology. *Biotechnol Adv* 27: 30–39.
12. Bagheri S, Julkapli NM, Yehye WA (2015) Catalytic conversion of biodiesel derived raw glycerol to value added products. *Energy Rev* 41: 113–127.
13. Johnson DT, Taconi KA (2007) The glycerin glut: options for the value-added conversion of crude glycerol resulting from biodiesel production. *Environ Prog* 26: 338–348.
14. Fan X, Chen R, Chen L, et al. (2016) Enhancement of alpha-ketoglutaric acid production from L-glutamic acid by high-cell-density cultivation. *J Mol Catal B: Enzym* 126: 10–17.
15. Appanna VD (1988) Alteration of exopolysaccharide composition in *Rhizobium meliloti* JJ-1 exposed to manganese. *Fems Microbiol Lett* 50: 141–144.
16. Kehres DG, Maguire ME (2003) Emerging themes in manganese transport, biochemistry and pathogenesis in bacteria. *Fems Microbiol Rev* 27: 263–290.
17. Jakubovics NS, Jenkinson HF (2001) Out of the iron age: new insights into the critical role of manganese homeostasis in bacteria. *Microbiology* 147: 1709–1718.
18. Culotta VC, Daly MJ (2013) Manganese complexes: diverse metabolic routes to oxidative stress resistance in prokaryotes and yeast. *Antioxid Redox Signal* 19: 933–944.
19. Appanna VD (1988) Stimulation of exopolysaccharide production in *Rhizobium meliloti* JJ-1 by manganese. *Biotechnol Lett* 10: 205–206.

20. Appanna VD, Preston M (1987) Manganese elicits the synthesis of a novel exopolysaccharide in an arctic *Rhizobium*. *Febs Let* 215: 79–82.
21. Otto C, Yovkova V, Barth G (2011) Overproduction and secretion of α-ketoglutaric acid by microorganisms. *Appl Microbiol Biotechnol* 92: 689–695.
22. Anderson S, Appanna VD, Huang J, et al. (1992) A novel role for calcite in calcium homeostasis. *Febs Let* 308: 94–96.
23. Hamel R, Appanna VD (2003) Aluminum detoxification in *Pseudomonas fluorescens* is mediated by oxalate and phosphatidylethanolamine. *BBA* 1619: 70–76.
24. Hamel R, Appanna VD, Viswanatha T, et al. (2004) Overexpression of isocitrate lyase is an important strategy in the survival of *Pseudomonas fluorescens* exposed to aluminum. *Biochem Biophys Res Commun* 317: 1189–1194.
25. Appanna VD, Gazs LG, Pierre MS (1996) Multiple-metal tolerance in *Pseudomonas fluorescens* and its biotechnological significance. *J Biotechnol* 52: 75–80.
26. Bradford MM (1976) A Rapid and sensitive method for the quantitation of microgram quantities of protein utilizing the principle of protein-dye binding. *Anal Biochem* 72: 248–254.
27. Alhasawi A, Leblanc M, Appanna ND, et al. (2015) Aspartate metabolism and pyruvate homeostasis triggered by oxidative stress in *Pseudomonas fluorescens*: a functional metabolomics study. *Metabolomics* 11: 1792–1801.
28. Frank J, Pompella A, Biesalski HK (2000) Histochemical visualization of oxidant stress. *Free Radical Biol Med* 29: 1096–1105.
29. Kuhn J, Müller H, Salzig D, et al. (2015) A rapid method for an offline glycerol determination during microbial fermentation. *Electr J Biotechnol* 18: 252–255.
30. Middaugh J, Hamel R, Jean-Baptiste G, et al. (2005) Aluminum triggers decreased aconitase activity via Fe-S cluster disruption and the overexpression of isocitrate dehydrogenase and isocitrate lyase: a metabolic network mediating cellular survival. *J Biol Chem* 280: 3159–3165.
31. Schägger H, von Jagow G (1991) Blue native electrophoresis for isolation of membrane protein complexes in enzymatically active form. *Anal Biochem* 199: 223–231.
32. Auger C, Appanna VD (2015) A novel ATP-generating machinery to counter nitrosative stress is mediated by substrate-level phosphorylation. *BBA* 1850: 43–50.
33. Auger C, Lemire J, Cecchini D, et al. (2011) The metabolic reprogramming evoked by nitrosative stress triggers the anaerobic utilization of citrate in *Pseudomonas fluorescens*. *Plos One* 6: e28469.
34. Alhasawi A, Castonguay Z, Appanna ND, et al. (2015) Glycine metabolism and anti-oxidative defence mechanisms in *Pseudomonas fluorescens. Microbiol Res* 171: 26–31.
35. Lietzan AD, Maurice MS (2013) Insights into the carboxyltransferase reaction of pyruvate carboxylase from the structures of bound product and intermediate analogs. *Biochem Biophys Res Commun* 441: 377–382.
36. Bignucolo A, Appanna VP, Thomas SC, et al. (2013) Hydrogen peroxide stress provokes a metabolic reprogramming in *Pseudomonas fluorescens:* enhanced production of pyruvate. *J Biotechnol* 167: 309–315.
37. Auger C, Appanna V, Castonguay Z, et al. (2012) A facile electrophoretic technique to monitor phosphoenolpyruvate-dependent kinases. *Electrophoresis* 33: 1095–1101.

38. Singh R, Lemire J, Mailloux RJ, et al. (2009) An ATP and oxalate generating variant tricarboxylic acid cycle counters aluminum toxicity in *Pseudomonas fluorescens*. *Plos One* 4: e7344.
39. Whittaker JW (2002) Prokaryotic manganese superoxide dismutases. *Methods Enzymol* 349: 80–90.
40. Igarashi T, Kono Y, Tanaka K (1996) Molecular cloning of manganese catalase from *Lactobacillus plantarum*. *J Biol Chem* 271: 29521–29524.
41. Tseng HJ, Srikhanta Y, McEwan AG, et al. (2000) Accumulation of manganese in *Neisseria gonorrhoeae* correlates with resistance to oxidative killing by superoxide anion and is independent of superoxide dismutase activity. *Mol Microbiol* 40: 1175–118.
42. Zeczycki TN, Menefee AL, Jitrapakdee S, et al. (2011) Activation and inhibition of pyruvate carboxylase from *Rhizobium etli*. *Biochem* 50: 9694–9707.
43. Adina-Zada A, Jitrapakdee S, Wallace JC, et al. (2014) Coordinating role of His216 in MgATP binding and cleavage in pyruvate carboxylase. *Biochem* 53: 1051–1058.
44. Yovkova V, Otto C, Aurich A, et al. (2014) Engineering the α-ketoglutarate overproduction from raw glycerol by overexpression of the genes encoding NADP-dependent isocitrate dehydrogenase and pyruvate carboxylase in *Yarrowia lipolytica*. *Appl Microbiol Biotechnol* 98: 2003–2013.
45. Lietzan AD, Maurice MS (2013) A substrate-induced biotin binding pocket in the carboxyltransferase domain of pyruvate carboxylase. *J Biolog Chem* 288: 19915–19925.
46. Li Q, Chen LS, Jiang HX, et al. (2010) Effects of manganese-excess on CO_2 assimilation, ribulose-1, 5-bisphosphate carboxylase/oxygenase, carbohydrates and photosynthetic electron transport of leaves, and antioxidant systems of leaves and roots in *Citrus grandis* seedlings. *BMC Plant Boil* 10: 42–10.
47. Mailloux RJ, Puiseux-Dao S, Appanna VD (2009) α-ketoglutarate abrogates the nuclear localization of HIF-1α in aluminum-exposed hepatocytes. *Biochimie* 91: 408–415.
48. Husain A, Sato D, Jeelani G, et al. (2012) Dramatic increase in glycerol biosynthesis upon oxidative stress in the anaerobic protozoan parasite *Entamoeba histolytica*. *Plos Negl Trop Dis* 6: e1831.
49. Kimura M, Ujihara M, Yokoi K (1996) Tissue manganese levels and liver pyruvate carboxylase activity in magnesium-deficient rats. *Biol Trace Elem Re*s 52: 171–179.

AIMS Press